






The effects of cyanobacterial biofilms on water transport and retention of natural building stones

Laurenz Schröer^{1,2}  | Tim De Kock³  | Sebastiaan Godts^{1,3,4}  | Nico Boon²  |
Veerle Cnudde^{1,5} 

¹PProGress, Department of Geology, Ghent University, Ghent, Belgium

²Center for Microbial Ecology and Technology (CMET), Department of Biotechnology, Ghent University, Ghent, Belgium

³Antwerp Cultural Heritage Sciences (ARCHES), University of Antwerp, Antwerp, Belgium

⁴Monuments Lab, Royal Institute for Cultural Heritage (KIK-IRPA), Brussels, Belgium

⁵Environmental Hydrogeology, Department of Earth Sciences, Utrecht University, Utrecht, The Netherlands

Correspondence

Laurenz Schröer, PProGress, Department of Geology, Ghent University, Krijgslaan 281 S8, 9000 Ghent, Belgium.
Email: laurenz.schroer@ugent.be

Funding information

Fonds Wetenschappelijk Onderzoek, Grant/Award Numbers: 11D4518N, 11D4520N, I013118N

Abstract

Water affects the susceptibility of stone to alteration by facilitating physical, chemical and biological weathering. Stone properties determine water transport and retention, but it is also expected that biofilms and extracellular polymeric substances could alter the water–stone relationship. A lot of research on this subject has been carried out on soils, but the effect on stones is understudied. For this reason, three sedimentary building stones, Ernzen, Euville and Savonnières, each with a different pore size distribution, were biofouled with cyanobacteria. Their relationship with the stone material was investigated by optical and electron microscopy, and the effect of cyanobacterial biofilms on water transport and retention was studied. The results showed that the cyanobacteria primarily colonize the building stones on the outer surface and have a limited effect on the water transport properties. They slightly reduced the capillary coefficient and drying rate of the stones, but enhanced the water content in the stone and increased water vapour sorption. They induced (near) hydrophobic conditions, but had no measurable effect on the gas permeability and water vapour diffusion. Moreover, swelling and shrinkage of the biofilms were observed, which could potentially induce physical weathering. It is expected that these changes could influence other forms of weathering, such as freeze–thaw weathering and salt weathering.

KEYWORDS

biodeterioration, biofouling, extracellular polymeric substances (EPS), heritage conservation, weathering

1 | INTRODUCTION

When bacteria colonize rocks, like natural building stones, they form biofilms or communities embedded in extracellular polymeric substances (EPS) (Flemming et al., 2016). The presence of biofilms and EPS might influence the stone properties. It is expected that biofilms and EPS alter the water transport and retention (Coombes & Naylor, 2012; Favero-Longo & Viles, 2020; McCabe et al., 2015; Schröer et al., 2021). Water is an important facilitator of stone alteration and deterioration. It enters stone by rainfall, infiltration (leakage or flooding) or capillary rise (Camuffo, 1995). It facilitates material dissolution (Cardell-Fernández et al., 2002) and transports and accumulates minerals such as damaging salts (Sawdy et al., 2008). Furthermore, water–ice phase transitions (Deprez et al., 2020) or the interaction of water with clay particles (Fontaine et al., 2015) can

induce mechanical stress and physical weathering. Water is also vital for biological growth, and its availability will determine the amount of biological colonization (Ortega-Morales et al., 2004; Ramírez et al., 2010).

Biofilms could alter the surficial capillary water transport, vapour diffusion and even change the wettability (Karimi et al., 2012; Polson et al., 2002; Warscheid, 1996; Warscheid & Braams, 2000; Warscheid et al., 1991). On soils, considerable progress has been made in understanding the effect of biofilms on the water–substrate relationship. There, an effect was detected of cyanobacterial biofilms on the hydraulic conductivity, clogging, water infiltration and water uptake (Colica et al., 2014; Eldridge, 2001; Malam Issa et al., 2009; Rossi et al., 2012). Their effect on building stones is not well studied, but there is an agreement that biofilms would affect the water inside the stones, and a conceptual model was designed by McCabe et al. (2015)

in which biofilms would make the stone increasingly non-breathable. Smith et al. (2011) suggested that algal biofilms tend to seal the surface and decrease the surface porosity and permeability of building stones. They proposed that algae biofilms aid moisture retention, facilitating higher water saturation degree to depth and even increase the dissolved salt penetration depth. Moreover, Coombes and Naylor (2012) detected reduced water absorption and evaporation rates on concrete covered with biochemical crusts, exposed to intertidal conditions. However, extensive experiments are missing on natural building stones, and it is unknown how biofilms affect moisture behaviour inside the stone. Increased knowledge on this topic is necessary to understand the influence of biofilms, as climate change and decreasing pollution could favour biological growth. For example, in Northern Ireland, building stones have already responded to environmental change, leading to the algal greening of the material (Smith et al., 2011; Viles & Cutler, 2012).

This research aims to experimentally identify the influence of EPS and biofilms on water transport and retention within natural stones. Therefore, the effect of biofilms will be assessed on capillary water absorption, drying rate, gas permeability, water vapour diffusion, water contact angle and water vapour sorption on three sedimentary stones: Ernzen, Euville and Savonnières. Half of the samples were biofouled with the cyanobacterium *Phormidium autumnale*. Their relationship with the substrate was studied using

spectrophotometry, (environmental) scanning electron and optical microscopy.

2 | MATERIALS AND METHODS

2.1 | Materials

Ernzen or Luxemburg sandstone is characterized by well to very well sorted fine to medium quartz grains cemented with sparitic or micro-sparitic iron-rich calcite or dolomite (Figure 1A) (Dusar et al., 2009; Molenaar, 1998). It is permeable and has an average porosity of 24.5%, although zones with a much lower porosity (<10%) exist (Molenaar, 1998). Ernzen contains a high amount of oversized secondary or mouldic porosity, and is affected by the occurrence of some laminae of detrital clays (Dusar et al., 2009; Molenaar, 1998).

Euville limestone is a French grainstone, which consists of 98% calcite and is built up by crinoid fragments overgrown by syntaxial calcite (Figure 1B). Euville has an average porosity between 10 and 20%. The pores are heterogeneously distributed and consist of macropores between the sparitic cement. Micropores occur within the particles, in between the sparite crystals, within micrite around the shell fragments and occasionally within micritized crinoid fragments and intraclasts (Dewanckele et al., 2014; Dusar et al., 2009; Fronteau, 2000).

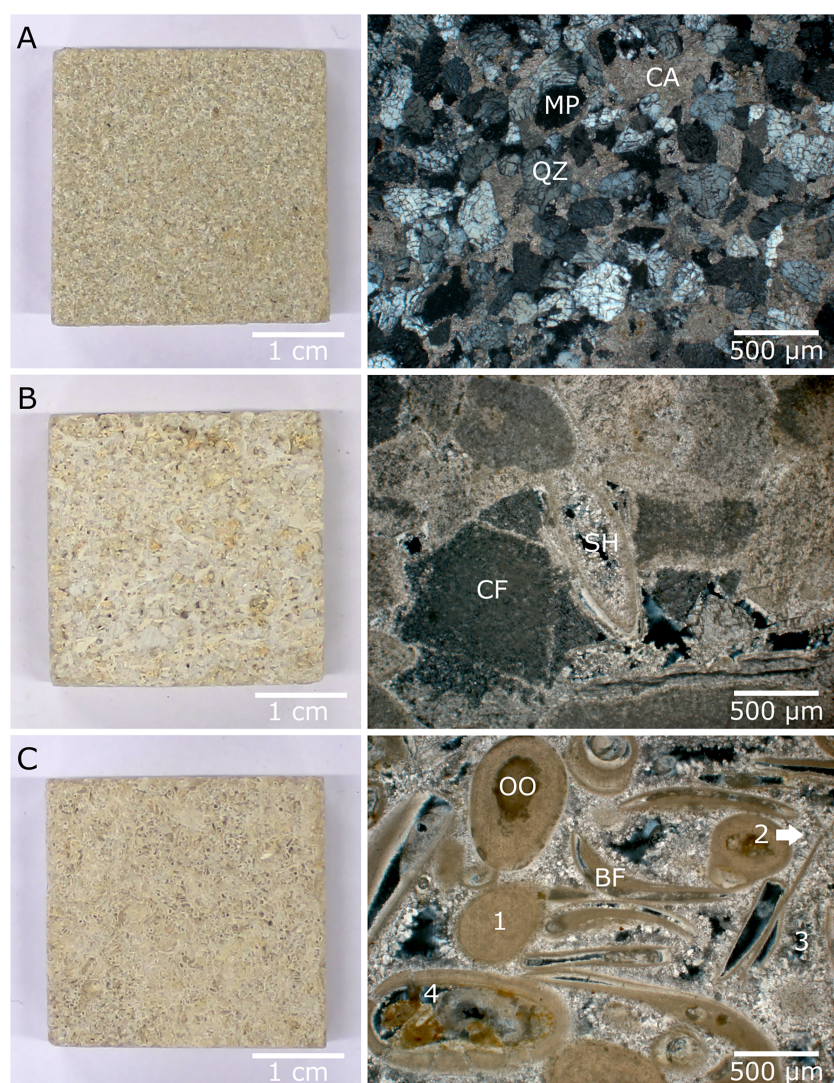


FIGURE 1 Macroscopic image (left) and thin sections under cross-polarized light (right) of (A) Ernzen sandstone, (B) Euville and (C) Savonnières limestone, with the thin sections showing the quartz grains (QZ) cemented by calcite (CA) on Ernzen and the presence of mouldic porosity (MP). Within Euville limestone, crinoid fragments (CF) can be identified, overgrown with syntaxial calcite cement and a shell fragment (SH) bordered with thin sparitic cement. The thin section of Savonnières limestone shows ooids (OO) and bivalve fragments (BF). The numbers refer to the pore types with (1) intragranular micropores, (2) intergranular micropores, (3) intergranular macropores and (4) intragranular macropores [Color figure can be viewed at wileyonlinelibrary.com]

Savonnières limestone is a French light beige grainstone (Dunham, 1962) or a rounded oosparite (Folk, 1962) (Figure 1C). It consists of 98.8% calcite with 70% sparite and 30% micrite, with dolomite as accessory mineral (Blows et al., 2003; Fronteau, 2000, 2010). It is a partially cemented limestone, dominated by mostly poorly preserved spherical to elliptical ooids (Figure 1C) (Dewanckele et al., 2014; Lebedev et al., 2014). Bivalve fragments are present, which are often locally concentrated, inducing a distinct layering and heterogeneity (Dewanckele et al., 2014; Lebedev et al., 2014; Roel et al., 2000). The total open porosity of Savonnières ranges between 22 and 41% (Fronteau, 2000). It has a complex pore system, with four types of distinguishable pores: (1) intragranular microporosity of the ooid walls; (2) intergranular microporosity between the sparitic cement; (3) triangular intergranular macroporosity in between the sparitic cement; and (4) intragranular macroporosity or mouldic porosity, induced by dissolution during diagenesis (Figure 1C). Larger macropores are only connected via micropores and can be considered as isolated regions. Besides the pores, microcracks and a secondary fracture porosity can be present (Derluyn et al., 2014).

These stones were chosen for their relevance as sedimentary building stones and their different porosities and pore structures. They are prominently used for buildings and monuments in north-western Europe. Within the Grand Duchy of Luxemburg, Ernzen sandstone is the most widespread and abundantly used building stone since the 12th century. It was also an important building stone in Belgium during the end of the 19th and beginning of the 20th century (Dusar et al., 2009). At the same time, Euville and Savonnières limestone were popular replacement and building stones. Within Belgium, they were by far the most popular French stone (De Kock et al., 2013; Dreesen et al., 2012; Dusar et al., 2009). Euville limestone was one of the most prestigious French stones (Dusar et al., 2009; Fronteau, 2000), and Savonnières limestone was used in the buildings of France, Germany, The Netherlands, Austria and Czechia, among others (Lorenz & Lehrberger, 2013).

The model organisms were freshwater cyanobacteria. *P. autumnale* ULC086 (also classified as CICALA 697) was acquired from the Belgian Co-ordinated Collections of Micro-Organisms (BCCM). They are filamentous and belong to the Oscillatoriales (Anagnostidis & Komárek, 1988). Freshwater types consist of simple, cylindrical, unbranched filaments (or trichomes) and form irregular colonies of more or less parallel filaments. Together with EPS, they adhere to the substrate and form mat-like structures (Strunecký et al., 2012). Cyanobacteria were chosen as they are one of the main

EPS producers (Rossi & De Philippis, 2015) and among the most important colonizers of building stones (Gaylarde et al., 2012; Golubić et al., 2015). *P. autumnale* occurs abundantly on natural building stones (Macedo et al., 2009; Ortega-Calvo et al., 1991; Rindi & Guiry, 2004; Tomaselli et al., 2000). The strain ULC086 was selected for its ability to form microbial mats, fast growth and durability. This strain was isolated from Ellesmere Island, Canada, out of the periphyton in a glacial stream (Strunecký et al., 2010).

2.2 | Methods

2.2.1 | Biofilm cultivation and biomass estimation

P. autumnale ULC086 was cultured in BG11+ medium. It grew in Erlenmeyers deposited in an incubator at 23°C, shaken at 120 rpm and on the bench of the laboratory, with temperatures between 13 and 17°C. All cultures were constantly illuminated by an LED strip, providing approximately 15–30 $\mu\text{mol m}^{-2} \text{s}^{-1}$ light. The same light intensity was maintained for all cultivation steps.

Biofilms were cultured on one side of Ernzen, Euville and Savonnières. Table 1 gives an overview of the biofouled samples used in the upcoming experiments, including their dimensions and how the biofilm was cultured. For each biofouled sample used to determine the water-transport properties, a non-biofouled, untreated sample was included to allow comparison. The cyanobacteria were partly disentangled by vortexing, and the stones were inoculated with a pipette. They grew on the bench to let them attach to the surface and were wetted by capillary uptake of water. Furthermore, every 2–3 days, BG11+ medium was added to the surface. It lasted mostly for a week until, at most locations, green discoloration was visible.

A dense biofilm was desired to study the effect on capillarity, drying, permeability, water vapour diffusion and sorption, and to make thin sections (one sample per building stone). After growth on the bench, these samples were placed on a water run-off setup in which the cyanobacteria and broth were constantly flown over the samples. This setup was based on De Muynck et al. (2009) (Figure 2). Above the setup, an LED strip was mounted. Growth lasted until the complete stone surface was covered in dark green biofilms. This took approximately 1–2 weeks. The time of biofouling was not fixed as the final biofilm coverage was the most important. Extra inoculation was sometimes necessary to accelerate growth. After biofilm

TABLE 1 Overview of the Ernzen, Euville and Savonnières samples biofouled with *P. autumnale*, including the dimensions, shape, number of replicates for each building stone and the process to induce biofouling. For each biofouled sample, a non-biofouled sample was included to allow comparison (except for [E]SEM and the optical microscopy studying thin sections)

Experiment	Dimensions	Replicates	Biofilm growth
SEM	2 × 2 × 1.5 cm (cylinder)	2×	Bench
ESEM	0.6 × 0.6 × 0.5 cm (cylinder)	1×	Bench
Optical microscopy	4.5 × 2.5 × 3 cm (rectangle)	3×	Bench + (run-off)
Capillarity, drying, permeability	5 × 5 × 5 cm (cylinder)	6×	Bench + run-off
Water vapour diffusion	8 × 8 × 2 cm (cylinder)	5×	Bench + run-off
Sorption	3 × 3 × 1 cm (rectangle)	6×	Bench + run-off
Contact angle	3 × 3 × 1 cm (rectangle)	3×	Bench

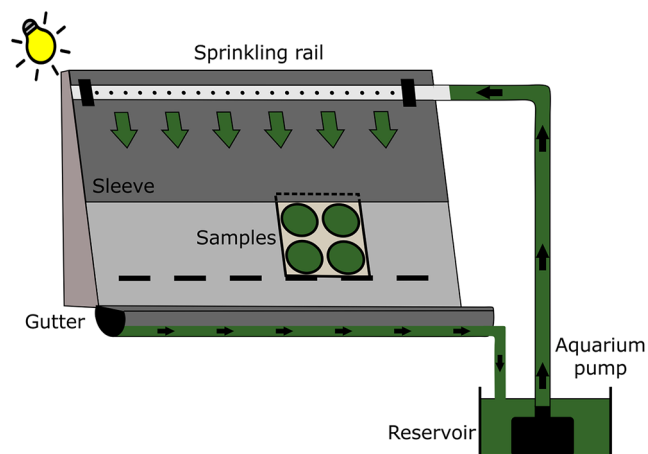


FIGURE 2 Illustration of the water run-off setup, where the cyanobacteria were constantly flowed over, in this case, cylindrical rocks mounted in a sample holder [Color figure can be viewed at wileyonlinelibrary.com]

development, the samples were submerged in tap water for 24 hours to remove salts deposited on the stones.

It is expected that the amount of biofilm will have an impact on the water transport properties. The amount of biofilm was estimated by measuring the colour difference (ΔE) before and after biofouling by spectrophotometry (Berger-Schunn, 1994). This is a simple, fast and non-destructive technique that allows robust biomass quantification on building stones (Prieto et al., 2004). Every sample used to study the water transport properties was photographed, and the superficial colours were determined before and after biofouling. The white balance of these pictures was corrected using a Mini ColorChecker Classic (MacBeth). A Konica Minolta CM-600d spectrophotometer with an 8 mm aperture determined the visible colour spectrum between 400 and 700 nm and provided quantitative colour data in the CIE L*a*b* colour space. The illuminant type D65, representing average daylight, was used. For the cylindrical samples of 5 cm (for capillarity, drying and permeability determination) and 8 cm diameter (for water vapour diffusion), respectively, five and nine measurements were taken, and the mean was determined. For the smaller biofouled samples, one measurement was performed in the centre.

2.2.2 | Microscopy

Biofouling was studied by scanning electron microscopy (SEM), environmental scanning microscopy (ESEM) and optical microscopy on thin sections.

SEM images were acquired on two biofouled Ernzen, Euville and Savonnières samples of $2 \times 2 \times 1.5$ cm. Images were acquired on the MIRA3 TESCAN SEM equipped with a field emission gun (FEG) from the Department of Geology (Ghent University, Belgium). All samples were carbon-coated, and both secondary (SE) and backscattered electron (BSE) images used a voltage of 5 kV. Before visualization, the cells were fixated in 2.5% glutaraldehyde in 0.1 N HEPES at a pH of 7.2 and dehydrated using an ethanol dehydration series of 50, 75, 90 and three times 100%.

ESEM was performed on the biofouled sample of $0.6 \times 0.6 \times 0.5$ cm of each stone without any additional sample

preparation. The biofilms were visualized in their hydrated state at the Royal Institute for Cultural Heritage (KIK-IRPA, Brussels, Belgium) using a Carl Zeiss EVO 15 LS SEM with LaB₆ filament. This was used as an ESEM at the extended pressure mode and after installing a cooling stage to regulate the temperature. Images were taken at 3°C, 20 kV using the backscatter detector. During the visualization, the relative humidity (RH) ranged between 10 and 100%, in which the specimen chamber had respectively a pressure between 76 and 760 Pa.

Thin sections were prepared to investigate endolithic growth. All biofouled stones were dried in the oven at 40°C, embedded with epoxy resin and cut perpendicular to the biofouled surface. The samples were polished with silicon carbide grinding paper (Stuers, Ballerup, Denmark), after which ± 30 μ m thin sections were prepared and analysed using a petrographic microscope (Axio Scope A1, Carl Zeiss Microscopy GmbH, Jena, Germany), both under plane- and cross-polarized light. Pictures were taken using the AxioCam MRC 5 camera and processed with AxioVision software (Zeiss, ver. 4.8.2) and ZEN 2.6 Lite.

2.2.3 | Water transport properties

After biofouling, the samples were dried in the oven at 40°C for 24 hours before starting the water transport experiments to comply with European standards. Preliminary tests showed that *P. autumnale* survived these conditions. Dried cells were rehydrated by adding water and showed motion under the optical microscope. Reinoculating dried biomass in BG11+ broth resulted in new growth.

The water transport properties of the biofouled samples were determined and compared with untreated samples. This approach allowed us to run each experiment simultaneously. However, it was necessary to include enough replicates to compare both groups of samples. Therefore, the number of replicates was chosen based on the European Standards. Furthermore, the significance of the observed differences between untreated and biofouled samples was determined by paired t-tests, in which *p*-values < 0.05 were regarded as significant.

The capillary water absorption was measured, based on the European Standard EN 1925 (1999), on twelve, $5 \times 5 \times 5$ cm cylindrical samples of Ernzen, Euville and Savonnières, which included for each stone six untreated and six biofouled samples. Ten minutes before the start, water (0.1–0.3 mL) was sprayed on the surface to allow rehydration and reactivation of the biofilms. The samples were weighed after rehydration and placed on a support within a box filled with 3 ± 1 mm water with the biofilms facing the bottom. The lowest centimetre of the sides was taped with parafilm to inhibit absorption from the sides. The samples were weighed after 1, 3, 5, 7, 10, 15, 20, 30, 45, 60, 240 and 1440 minutes. For Euville, additional measurements were performed after 75, 90 and 120 minutes, due to the slower capillary water absorption. With these results, the capillary coefficient was determined, which represents the initial or unsaturated capillary absorption rate.

After absorbing water by capillarity for 24 hours, the samples were immersed in water for four days and the drying rate was determined. Hereafter, they were packed with parafilm and tape, leaving one side exposed to the environment. For the biofouled samples, this was the side covered with biofilms. They were dried in a climatic

chamber at 23°C and 50% RH as described by the European Standard EN 16322 (2013). Their weight was measured every 20 minutes for the first hour, every hour during the next seven hours and twice a day, with at least six hours in between for the rest of the experiment on working days. During the weekend, one measurement was performed. The results were presented as the water content, expressed in m% of the water compared to the dry material over time in hours. The constant drying rate was determined during the first drying phase, by linear regression, just like the start of the second phase and the critical moisture content.

When a stable weight was reached, the permeability was determined with a mini-permeameter “Tiny Perm II” (New England Research Inc., White River Junction, VT). The Tiny Perm was mounted in a static upright position to provide reproducible testing, and three measurements were performed for each sample. The resulting Tiny Perm value (*TP*) was linked to the gas permeability *K* (mD) (Filomena et al., 2014).

The water vapour diffusion was determined according to the wet cup method (EN ISO 12572, 2016) on 30 cylindrical samples of 8 × 8 × 2 cm, ten of each stone, of which half were biofouled. Within the cup, RH of 94% was established by a saturated KNO₃ solution (400 g/L). A climatic chamber established the surrounding conditions of 23°C and 50% RH. The rate of vapour transmission at steady state was determined by periodic weightings and the water vapour resistance factor was determined according to EN ISO 12572 (2016), using the value 1.9 × 10⁻¹⁰ kg/(m s Pa) for the water vapour permeability.

The wettability was determined for six rectangular samples, 3 × 3 × 1 cm of Ernzen, Euville and Savonnières, of which half were slightly biofouled to maintain a straight surface to not hinder the analysis. Static water contact angle (WCA) measurements were performed in triplicate per sample. They were determined by a Krüss Drop Shape Analyzer (DSA25S, Krüss GmbH, Germany) optical system. After a 2 µL droplet of distilled water was placed on the sample surface, a video (with a rate of 25 fps) was recorded and stored using a monochrome interline CCD video camera, PC-based acquisition and data processing. Subsequently, the WCA was automatically measured on each frame containing the water droplet on the surface using the computer software provided with the goniometer applying the Laplace–Young curve fitting method. All measurements were carried out under ambient air and temperature conditions. The stones quickly absorbed the water droplet and, for this reason, it was not possible to determine the static contact angle according to European standard EN 15802 (2010). During absorption, the contact angle of a water droplet decreased to zero, when it disappeared (Lee et al., 2016). The WCA was determined on the first frame after the droplet touched the surface, assuming that at that moment, absorption did not start. Furthermore, based on the number of frames, the time until complete absorption was determined.

Sorption was determined by the desiccator method (EN ISO 12571, 2013) on 36 rectangular samples of 3 × 3 × 1 cm, twelve of each stone, of which half were biofouled. The samples were placed in a series of desiccators with increased RH at ambient temperature. The following theoretical RHs were established above saturated solution in equilibrium: 0% (silica gel), 33% (MgCl₂), 53% ([MgNO₃]₂•6H₂O), 85% (KCl) and 94% (KNO₃). Temperature and RH were monitored during the experiment. The samples were weighed once a week until

an equilibrium for each RH was reached. After determining the moisture content at each RH, the sorption curve was drawn.

3 | RESULTS

3.1 | Biofilm cultivation and measurement

P. autumnale developed dark green biofilms, resulting in a colour difference (ΔE) (Table 2). Figure 3 visualizes the biofouling of representative samples by presenting white-balanced images and the ΔE of that specific sample. The highest colour difference was observed on the stones with biofilm cultured by the water run-off setup. For the different stones, the mean ΔE ranged between 45.71 and 52.80 for the samples for water vapour diffusion and sorption. A lower amount of biofilm developed on the samples later used for capillary absorption, drying and permeability measurements, in which the mean value ranged between 27.30 and 46.01. The colour difference of the surface for the wettability samples ranged between 3.54 and 20.37 (Table 2).

The coverage was not homogenous, especially when less biofilm was present ($\Delta E < 40$) (Figures 3A and D). Moreover, intermittent drying of extensively biofouled stones caused the partial detachment and exfoliation of the biofilm from the surface (Figures 3B and C). These partially detached biofilms were not removed but could fall off during the experiments, which was mainly an issue for Euville and

TABLE 2 Colour difference (ΔE) induced after biofouling Ernzen, Euville and Savonnières before the water transport experiments, displaying the mean colour difference (ΔE_{mean}) and the sample with the minimal (ΔE_{min}) and maximal colour difference (ΔE_{max}). ΔE_{mean} and its standard deviation were retrieved from six samples prepared for capillarity + drying + permeability (five measurements per sample), five samples for water vapour diffusion (nine measurements per sample), six samples for the sorption experiments (one measurement per sample) and was based on three samples for the wettability (one measurement per sample)

Stone	ΔE_{mean}	ΔE_{min}	ΔE_{max}
Capillary absorption + drying + permeability			
Ernzen	27.30	25.23	31.69
Euville	31.36	25.58	36.95
Savonnières	46.01	37.71	51.30
Water vapour diffusion			
Ernzen	45.71	41.15	48.69
Euville	47.68	44.51	51.16
Savonnières	50.20	45.72	54.42
Sorption			
Ernzen	46.32	31.20	50.21
Euville	52.50	42.79	58.88
Savonnières	52.80	40.99	57.88
Wettability			
	Sample 1	Sample 2	Sample 3
Ernzen	9.48	7.88	14.84
Euville	6.75	3.54	10.55
Savonnières	18.70	16.87	20.37

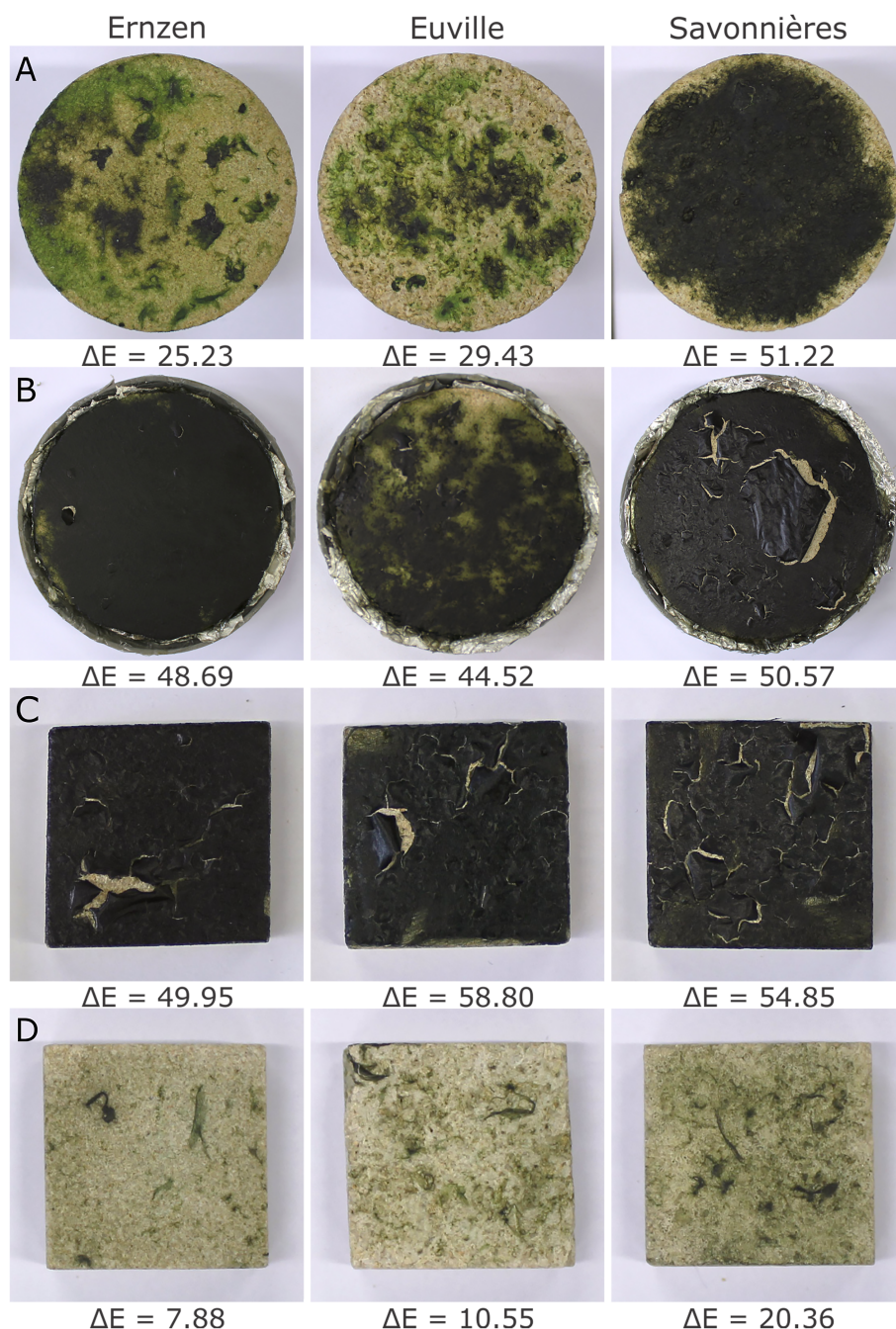


FIGURE 3 White balanced images of representative biofouled samples Ernzen, Euville and Savonnières used to determine (A) capillarity, drying and permeability, (B) water vapour transport, (C) water sorption and (D) wettability. The ΔE of each sample is written underneath, with ΔE of (A) and (B) the mean of five and nine measurements, respectively [Color figure can be viewed at wileyonlinelibrary.com]

Savonnières samples. For this reason, less biofilm was cultured on the stones to measure the capillary absorption.

3.2 | Microscopy

Individual cells of *P. autumnale* were recognized by electron microscopy. They were attached to the surface, in which their filaments could follow surface irregularities (Figure 4A) or were attached by discrete portions of EPS (Figure 4B). In case of high concentrations, they formed biofilms, in which the cells were more or less aligned on sheets of EPS (Figure 4C). They mainly covered the surface, sealed the pores (Figure 4D) or locally entered pores and grew on the pore wall. Cracking of the biofilms could cut through the individual cells (Figures 4C and D). No fungi or other algae were present, but at higher magnifications (1000 \times and more as in Figures 4A and B), other rod-shaped or coccoid bacteria were found on the biofilm. No signs of deterioration,

such as pitting or dissolution features, were detected. There were no indications that these cyanobacteria grew endolithic. Although, along with the cells and the EPS, some granular precipitates were present, appearing brighter on the BSE images, suggesting an inorganic composition. Similar observations were made by imaging the biofilms with optical microscopy.

The ESEM images revealed some cracked biofilms and filaments. Compared to the SEM images, more EPS was visible. Furthermore, ESEM showed that when the RH decreased, the biofilm immediately shrunk, while an RH increase caused the biofilm to swell. The effect of changing RH is presented in Figure 5 on Euville. The effect was also recorded in a video and added to the online Supplementary Material. Here, the RH changed from 10% towards 100% in steps of 10% over a total period of approximately ten minutes. This shows that the biofilm swelled in steps, almost synchronizing the increase in RH. Swelling/shrinking of a biofilm occurred over the whole range between 100 (Figure 5A) and 10%

FIGURE 4 SEM image of biofouled (A) Ernzen, (B) Euville and (C, D) Savonnières covered with elongated cyanobacteria identified as *P. autumnale* embedded in an EPS matrix, which was cracked at some locations. Besides the cyanobacteria, small rod-shaped bacteria were present covering the stone surface, cyanobacteria and EPS. Attached to the cells and EPS, inorganic precipitates were present, most likely salts from the growth medium (based on BSE images, not shown here)

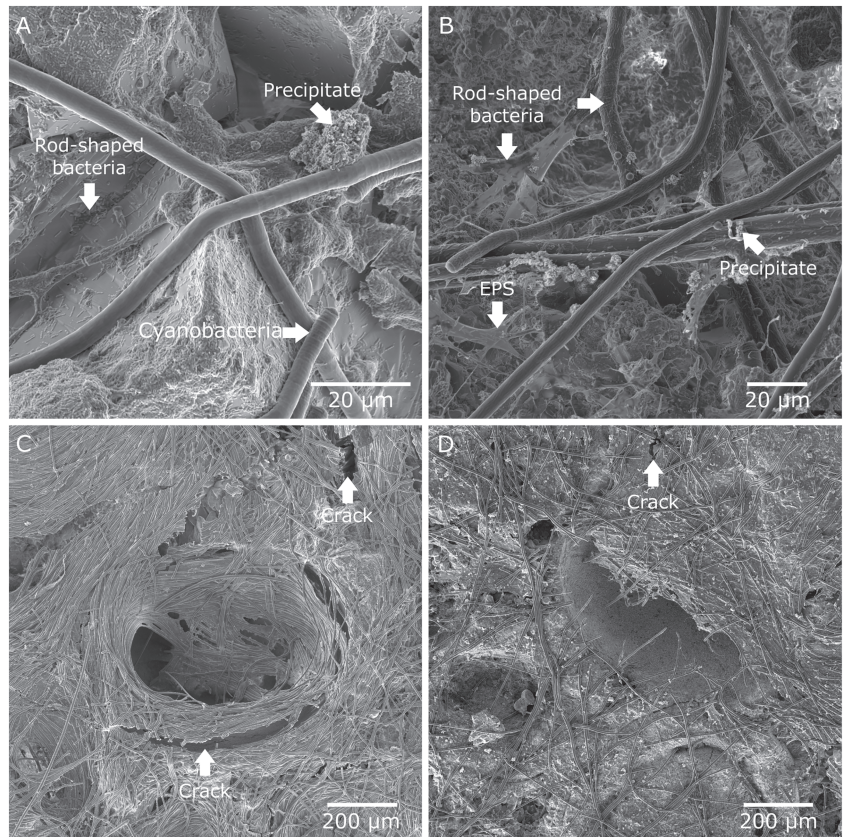
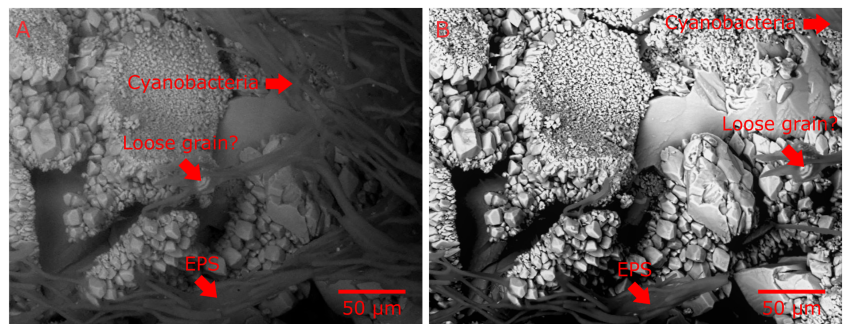


FIGURE 5 ESEM image of biofouled Euville at an RH of (A) 100% and (B) 10% showing the shrinkage of the cyanobacteria and the EPS. The biofilm in the right corner moves almost out of the field of view, during which it takes a potential loose grain with it [Color figure can be viewed at wileyonlinelibrary.com]



RH (Figure 5B). At an RH of 10%, the biofilm almost disappeared out of the field of view. Increasing the RH caused the biofilm to expand until it reached a similar state as Figure 5A. During this swelling–shrinkage cycle, it was observed that the biofilm moved inorganic material, something like a grain, transporting it over a distance of approximately 150 µm.

The examination of the thin sections visualized the biofilms covering the stone surfaces of each sample. On most occasions, the biofilms were partly attached to the surface while they covered the grain but spanned over the pores (Figure 6A). However, sometimes they also colonized the pores and were attached to the inside (Figure 6B). Similar observations were made by SEM (Figure 4) and ESEM (Figure 5). The penetration was still very limited, and these pores were still a part of the outer edge of the stones. No extensive endolithic colonization was detected, except within the two Euville samples on which the biofilms grew solely on the bench. The thin sections of those samples revealed biofilms inside the stone samples until a depth of at least 1 mm (Figures 6C and D).

3.3 | Water transport properties

Biofouled samples have a reduced capillary water absorption compared to untreated samples (Figure 7). The biofouled samples of Ernzen, Euville and Savonnières experienced a mean decrease of the capillary coefficient of 15.63, 15.89 and 25.02%, respectively, compared to the untreated samples (Table 3). However, only for Ernzen was this difference significant, with a *p*-value of 0.0353. For Euville and Savonnières, these were 0.2744 and 0.0583, respectively. Variability was most prominent for the untreated samples as biofouled samples have a lower standard deviation of the capillary coefficients.

Biofouled samples obtained their capillary moisture content later in the absorption process, compared to untreated samples. This illustrates the increased duration of capillary absorption for all stones (Figure 7). The paired *t*-test showed that the effect of biofouling was significant for all stones. The *p*-values for Ernzen, Euville and Savonnières were 0.0113, 0.0228 and 0.0043, respectively. The

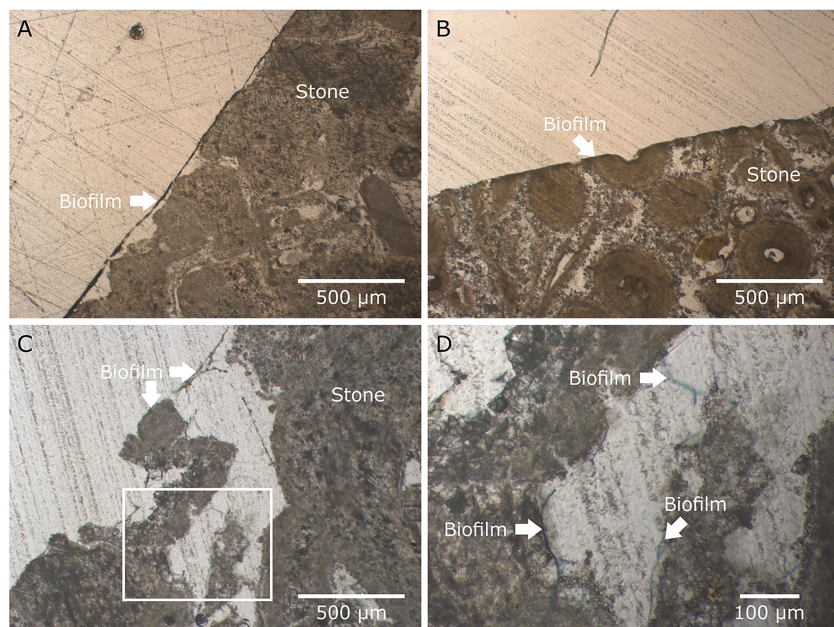


FIGURE 6 Thin sections under cross-polarized light through the biofouled edge of (A) Euville and (B) Savonnières, illustrating the biofilm covering the stone surface, (A) spanning over the pores or (B) following the surface including local depressions induced by the pores; (C), with detail (D), indicated by the box, shows the biofilms at the edge of the stone and inside the pores [Color figure can be viewed at wileyonlinelibrary.com]

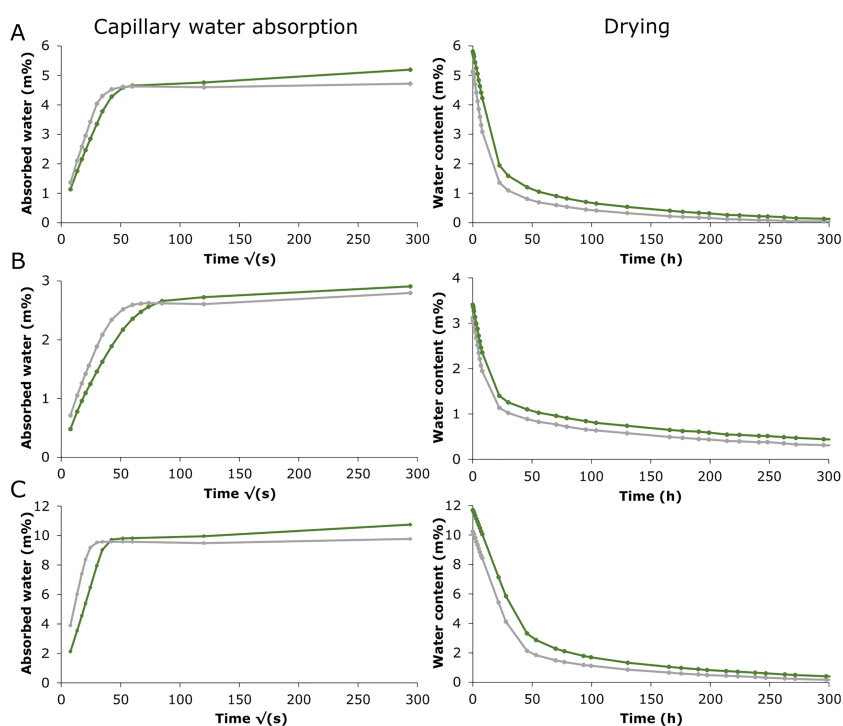


FIGURE 7 Mean capillary water absorption as a function of time (left) and mean water content during drying at 23°C and 50% RH (right) of (A) Ernzen, (B) Euville and (C) Savonnières with the blanks in grey and the biofouled samples in green [Color figure can be viewed at wileyonlinelibrary.com]

TABLE 3 Mean coefficient of capillarity (C_{mean} [$\text{g m}^{-2} \text{s}^{-1/2}$]), including standard deviation, with minimum (C_{min} [$\text{g m}^{-2} \text{s}^{-1/2}$]) and maximum (C_{max} [$\text{g m}^{-2} \text{s}^{-1/2}$]), measured values of each untreated and biofouled stone

Stone	Treatment	C_{mean} ($\text{g m}^{-2} \text{s}^{-1/2}$)	C_{min} ($\text{g m}^{-2} \text{s}^{-1/2}$)	C_{max} ($\text{g m}^{-2} \text{s}^{-1/2}$)
Ernzen	Untreated	124.63 ± 27.78	80.16	149.70
	Biofouled	105.15 ± 15.97	86.89	124.59
Euville	Untreated	60.56 ± 14.69	42.11	80.79
	Biofouled	50.94 ± 11.26	40.35	65.55
Savonnières	Untreated	306.08 ± 55.87	232.02	377.42
	Biofouled	229.50 ± 27.94	181.68	261.38

capillary moisture content of the biofouled samples was slightly higher compared to the untreated ones (Table 4), but the difference was not significant.

After reaching the capillary moisture content, the biofouled samples of Ernzen and Savonnières absorbed an additional 4.54 and 3.59 times the amount of water, respectively, compared to their untreated

TABLE 4 Mean values and standard deviations of untreated and biofouled Ernzen, Euville and Savonnières describing the duration of the capillary water absorption ($T_{\text{capillary abs.}}$ [min.]), the capillary moisture content ($M_{\text{capillary}}$ [m%]) and the amount of absorbed water by diffusion ($M_{\text{diffusion}}$ [m%]) until 24 hours after the start of the experiment

Stone	Treatment	$T_{\text{capillary abs.}}$ (min.)	$M_{\text{capillary}}$ (m%)	$M_{\text{diffusion}}$ (m%)
Ernzen	Untreated	23.74 ± 10.36	4.59 ± 0.45	0.13 ± 0.05
	Biofouled	35.69 ± 8.55	4.61 ± 0.52	0.59 ± 0.06
Euville	Untreated	39.06 ± 16.33	2.56 ± 0.22	0.23 ± 0.04
	Biofouled	78.83 ± 25.21	2.67 ± 0.34	0.24 ± 0.02
Savonnières	Untreated	10.52 ± 3.04	9.48 ± 0.98	0.29 ± 0.05
	Biofouled	21.54 ± 2.93	9.71 ± 2.93	1.04 ± 0.12

TABLE 5 Mean drying characteristics, including standard deviations, of untreated and biofouled Ernzen, Euville and Savonnières at 23°C and 50% RH. Constant drying rate is expressed as water loss (mg) for each gram of stone per hour. The critical moisture content is given in m% of water within each building stone

Stone	Treatment	Constant drying rate ($\text{mg g}^{-1} \text{h}^{-1}$)	Critical moisture content (m%)	Time constant drying period (h)
Ernzen	Untreated	-2.65 ± 0.18	3.44 ± 0.32	6.61 ± 0.06
	Biofouled	-2.00 ± 0.20	2.93 ± 1.31	15.24 ± 9.69
Euville	Untreated	-1.49 ± 0.22	2.10 ± 0.31	6.81 ± 0.22
	Biofouled	-1.34 ± 0.17	2.49 ± 0.24	6.94 ± 0.97
Savonnières	Untreated	-2.20 ± 0.20	4.63 ± 0.59	25.43 ± 4.02
	Biofouled	-2.11 ± 0.13	6.25 ± 0.31	26.07 ± 4.30

TABLE 6 Mean Tiny Perm (TP) value with the corresponding gas permeability (K [mD]) and mean water vapour resistance (μ), with their standard deviations, for the untreated and biofouled Ernzen, Euville and Savonnières

Stone	Treatment	TP value	K (mD)	μ
Ernzen	Untreated	10.53 ± 0.16	783.3 ± 338.6	21.04 ± 1.66
	Biofouled	10.61 ± 0.12	601.3 ± 185.0	21.24 ± 3.25
Euville	Untreated	10.76 ± 0.26	471.5 ± 345.8	41.53 ± 2.67
	Biofouled	10.76 ± 0.29	481.5 ± 327.7	36.74 ± 5.92
Savonnières	Untreated	10.19 ± 0.13	1976.9 ± 681.4	21.53 ± 0.63
	Biofouled	10.13 ± 0.15	2378.8 ± 844.2	21.27 ± 0.90

counterparts. This was significant as the corresponding p -values were <0.001. No significant difference was detected within Euville (Table 4). After 24 hours, the biofouled samples absorbed more water, adding overall almost 1 m% water for Savonnières, 0.48 m% for Ernzen and 0.11 m% for Euville (Table 4). During the measurements, some biofilms detached from the surface after removing the non-absorbed water before every weighing. Biofilm removal was most pronounced for Savonnières samples and could reduce the observed effect of the biofilm.

Before drying, after 24 hours of capillary water uptake and four days of full immersion, the water content of the biofouled samples was higher. The mean water content of the untreated and biofouled Ernzen was 5.14 ± 0.39 and 5.81 ± 0.34 m%, respectively; 3.12 ± 0.26 and 3.41 ± 0.31 m% for Euville and 10.24 ± 0.92 and 11.70 ± 0.75 m% for Savonnières. These results differed, according to the paired t -test, significantly for Ernzen with a p -value of 0.0003. For Euville and Savonnières, the difference was almost significant with a p -value of 0.0692 and 0.068, respectively.

Two drying periods can be distinguished in Figure 7, of which the results are presented in Table 5. The mean constant drying rate was lower for all biofouled building stones. The largest difference was

measured for Ernzen, at -2.65 and $-2.00 \text{ mg g}^{-1} \text{h}^{-1}$ for the untreated and biofouled stones, respectively. The difference was only significant for Ernzen, with $p = 0.0066$.

The constant drying phase of biofouled stones lasted longer but remained very similar for Euville and Savonnières (Table 5). The differences in critical moisture content for the untreated and biofouled stones were not consistent (Table 5). Moreover, they were not significant. An exception was Savonnières, where the biofouled samples had an increased moisture content of importance, with a p -value of 0.0011. The difference for Euville was still relatively significant, as the p -value was 0.0535, which is only negligibly greater than 0.05.

During the second phase, the drying rate declined. After 21, 31 and 23 days, respectively, Ernzen, Euville and Savonnières reached a stable weight, leaving <0.05 m% of residual water, with a negligible difference between the untreated and biofouled stones.

The values of the gas permeability were not consistent, highly variable and no significant difference could be determined (Table 6). Moreover, the water vapour resistance factor was similar for the untreated and biofouled samples of Ernzen and Savonnières (Table 6). There was a slight difference for Euville as the mean water vapour factor for the untreated and biofouled samples was 41.53 and 36.74,

respectively. However, none of the results were significantly different, with p -values for Ernzen, Euville and Savonnières of 0.5898, 0.13 and 0.6648, respectively.

Moreover, biofouled stones had a higher WCA immediately after contact with the surface (Table 7, Figure 8). The difference was the largest on Savonnières, followed by Euville and Ernzen. The p -values of Ernzen, Euville and Savonnières were 0.0003, <0.0001 and <0.0001, respectively. These values show an important influence in the surface behaviour of biofouled samples.

Even though biofouling increased the WCA, the droplets were still quickly absorbed (Table 7) inside the stone, and the biofilms swelled sometimes after adding the water. Biofouled Ernzen and Euville absorbed the water at a slower rate, while biofouled Savonnières absorbed the water slightly faster, compared to the untreated samples. The differences were only significant for Ernzen, in which the p -value was 0.0196, compared to 0.0855 for Euville and 0.6065 for Savonnières. The rate of the droplet absorption differed between the measurements. It could reach a factor of 10 for the same stone type at the same condition (e.g. Euville 10.28 vs. 0.88 s) and resulted in very high standard deviations.

Furthermore, biofouled samples acquired more hygroscopic water by vapour sorption compared to their untreated counterparts (Figure 9, Table 8).

At an RH of 37.1%, the absorbed moisture was similar for Ernzen and Euville, while a larger difference was measured for Savonnières (Table 8). At an RH of 98.2%, the measurements obtained after one week were included. This was before equilibrium, but afterwards, the samples became contaminated with mould. Paired t -tests showed that the difference between the untreated and biofouled samples was often significant. Biofouled Ernzen sorbed significantly more water at an RH of 91.5% (p -value = 0.0498). At other RHs, this difference was

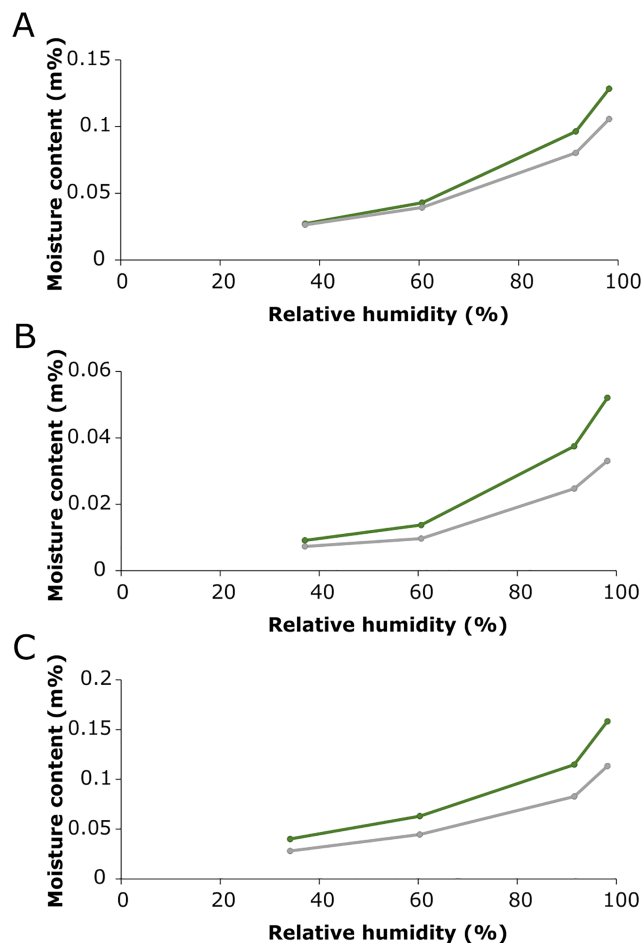


FIGURE 9 Sorption curve showing the mean moisture content at a certain RH of untreated (grey) and biofouled (green) (A) Ernzen, (B) Euville and (C) Savonnières [Color figure can be viewed at wileyonlinelibrary.com]

TABLE 7 Measured WCA at the moment when the droplet touched the surface of the untreated and biofouled Ernzen, Euville and Savonnières, including the mean WCA (WCA_{mean} [°]), of nine measurements, the minimum (WCA_{min} [°]) and maximal value (WCA_{max} [°]), mean absorption time ($T_{abs. mean}$ [s]), including the minimal ($T_{abs. min}$ [s]) and maximum ($T_{abs. max}$ [s]) time. The mean values are represented with their standard deviations

Stone	Treatment	WCA_{mean} (°)	WCA_{min} (°)	WCA_{max} (°)	$T_{abs. mean}$ (s)	$T_{abs. min}$ (s)	$T_{abs. max}$ (s)
Ernzen	Untreated	53.7 ± 11.3	39.3	73.6	1.56 ± 1.48	0.40	4.48
	Biofouled	85.7 ± 10.2	68.8	105.1	4.21 ± 1.57	1.32	5.56
Euville	Untreated	45.6 ± 7.9	29.4	51.4	1.37 ± 0.89	0.52	2.08
	Biofouled	93.3 ± 8.9	80.3	108.4	3.61 ± 2.90	0.88	10.28
Savonnières	Untreated	47.1 ± 6.5	39.9	57.6	1.31 ± 0.97	0.36	2.76
	Biofouled	103.5 ± 14.6	83.4	128.8	1.16 ± 0.49	0.44	1.96

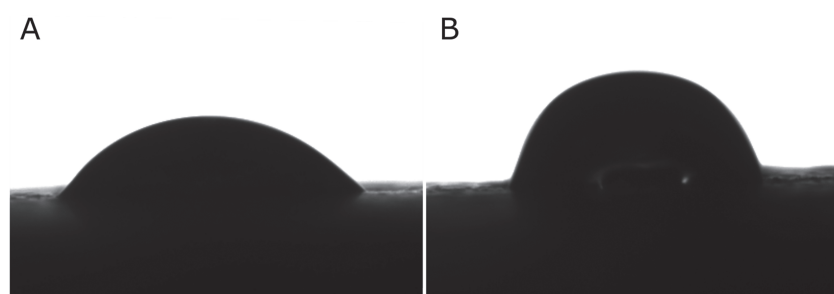


FIGURE 8 Water droplet immediately after contact with (A) untreated Savonnières limestone and (B) biofouled Savonnières limestone

TABLE 8 Mean moisture content and standard deviation (m%) acquired by hygroscopic suction of untreated and biofouled Ernzen, Euville and Savonnières at each RH (%)

Stone	Treatment	Relative humidity (%)			
		37.1	60.6	91.5	98.2**
Ernzen	Untreated	0.026 ± 0.004	0.039 ± 0.006	0.080 ± 0.013	0.106 ± 0.019
	Biofouled	0.027 ± 0.002	0.043 ± 0.003	0.096 ± 0.006	0.128 ± 0.008
Euville	Untreated	0.007 ± 0.001	0.010 ± 0.002	0.025 ± 0.004	0.033 ± 0.006
	Biofouled	0.009 ± 0.001	0.014 ± 0.002	0.037 ± 0.008	0.052 ± 0.011
Savonnières	Untreated	0.028 ± 0.006*	0.045 ± 0.008	0.083 ± 0.014	0.113 ± 0.021
	Biofouled	0.040 ± 0.004*	0.063 ± 0.005	0.115 ± 0.038	0.158 ± 0.041

*Mean moisture content at an RH of 34.1 instead of 37.1.

**Measurement after one week as afterwards the biofouled samples were contaminated with mould.

TABLE 9 Summary of the effect of cyanobacteria on the studied water transport properties

Property	Impact biofilm	Significance
Capillary coefficient	Decrease	Significant for Ernzen (nearly for Savonnières)
Water absorption at atmospheric pressure	Increase	Significant for Ernzen (nearly for Euville and Savonnières)
Drying rate	Decrease	Only significant for Ernzen
Gas permeability	Not measurable	Not significant
Water vapour diffusion	Not measurable	Not significant
Water contact angle	Increase	Significant for all studied stones
Water vapour sorption	Increase	Variable significance

less meaningful yet more important at 98.2%, with a p -value of 0.0547. Biofouled Euville limestone contained significantly more water at 60.6, 91.5 and 98.2% RH, with p -values of 0.0143, 0.0141 and 0.0187, respectively. At an RH of 37.1%, the difference was almost notable, with a p -value of 0.08. For Savonnières, a significant difference was only present at an RH of 34.1 and 60.6%, with a p -value of 0.0143 and 0.0079, respectively. At higher RHs of 91.5 and 98.2%, the p -value rose again to 0.1232 and 0.0785, respectively.

4 | DISCUSSION

Biofilms and EPS of *P. autumnale* covering Ernzen, Euville and Savonnières impacted water transport and retention. A summary of the results is presented in Table 9. The changes were limited and not always significant within the given experimental procedure. However, the effect on the biofilm was often similar on the different rock types and thus consistent. Biofouling reduced the capillary water absorption at the surface of the stones. It was most prominent on Savonnières limestone, which could be explained by the high amount of biofouling compared to the other stones (Table 2). The increased water content is related to the additional amount of water absorbed by the biofilm itself. The decrease in capillary absorption does not agree with the previous findings of Warscheid et al. (1991). They suggested that biofilms increased the rate of capillary water uptake after comparing the capillarity of a biofouled outer wall with a biofilm-free inner wall.

Moreover, a relatively low amount of biofilms induced (near) hydrophobic conditions. This was caused by EPS, which mainly consists of polysaccharides, nucleic acids, lipids and proteins. These

biomolecules have different hydrophobic or hydrophilic properties and thus can change the wettability of a surface. Moreover, biofilms affected the contact angle of a surface by changing the surface chemistry, roughness and re-entrant topography (Epstein et al., 2011; Tanaka et al., 2019). Increased water contact angles were also examined due to carbonatogenic bacteria (Elert et al., 2021) and *Bacillus subtilis* (Epstein et al., 2011). Polson et al. (2002, 2010) detected a change in wettability on quartz by a bacterial–fungal consortium that made the surface hydrophobic, while an algal consortium left the surface hydrophilic. Its effect could be limited as the water droplets were still quickly absorbed. Moreover, the duration of absorption was highly variable. This could be related to the small droplet volume, the different wettability of locally present biomolecules, local inhomogeneities of the building stones or incomplete colonization on the surface, which was overall limited to the outer surface.

The increase in water retention was illustrated by a reduced drying rate and increased sorption of hygroscopic water. The results agree with Coombes and Naylor (2012) and Warscheid et al. (1991). This was expected from EPS, as it protects bacteria from desiccation (Rossi & De Philippis, 2015). The enhanced sorption of the biofouled samples is a result of the hygroscopic behaviour of the biofilm as observed under ESEM (Figure 5), where the size of the biofilm was directly related to the surrounding RH. No measurable effect could be determined on gas permeability and water vapour diffusion. Together with Figure 7, this shows that the second drying phase was not heavily hindered by the biofilms.

In their review, Warscheid and Braams (2000) suggested a potential increase in capillary water uptake as biofilms narrow rock pores. However, the biofilms seemed to obstruct water absorption and evaporation. As the pores of Ernzen, Euville and Savonnières are in the

typical capillary range (radius 0.1–1000 μm), the observed decrease in absorption rate and increased water retention were expected by the narrowing surficial pores (Siegesmund & Snethlage, 2014). Pore clogging and sealing of the superficial pore space were observed by microscopy (Figure 4), which agrees with Smith et al. (2004, 2011). Furthermore, the decreased absorption could also be influenced by the induced hydrophobicity.

These experiments were not hindered by contamination besides the sorption experiment at an RH of 98.2%. Contamination with heterotrophic bacteria might occur as visualized in Figure 4, but compared to the cyanobacteria, their size was negligible. Cultivating biofilms on the stones and estimating their amount by spectrophotometry was successful. However, a lot of variation in the water transport properties and degree of biofouling occurred, hindering quantitative analyses. Overall, *P. autumnale* grew the easiest on Savonnières, where it resulted in the fast development of dark green biofilms with mostly higher ΔE (Table 2). This was most likely related to the bioreceptivity. Growth was limited to the surface (except for limited endolithic growth visible on some thin sections of Euville). Some of the biofilms were detached before and during the experiments, which might have reduced their impact during the experiments. This was most likely caused by the limited attachment of the biofilms on the surface and the cracks, both macroscopically (Figure 3) and microscopically (Figures 4 and 5), which were most likely related to shrinkage during drying. However, no intense drying occurred before acquiring ESEM imaging, suggesting that it could rupture easily.

Generally, the data represented here confirmed the conceptual model of McCabe et al. (2015). They proposed that biofilms alter the stone surface, leading to more effective trapping of moisture. The moisture ingress would be slowed down due to a lower capillary absorption rate, while moisture loss would be more difficult. They also suggested a decrease in permeability, although this could not be observed.

Moreover, the effect of biofilms on building stones is comparable with previous findings of soil research in arid to semi-arid regions. However, the effect of biofilms, described as 'biocrusts', on water infiltration and hydrology remains controversial (Xiao et al., 2019). The results agreed with previous findings, where the EPS matrix absorbed and delayed water movement by expanding and becoming less fibrous. There, the EPS acted as a buffer for the cells and also decreased or at least delayed the evaporation of water (Mager & Thomas, 2011; Potts, 2001). This reduced the evaporation in soils (Xiao et al., 2010) and could increase the water-holding capacity (Adessi et al., 2018; Rosenzweig et al., 2012), which was also detected (by Malam Issa et al., 2009) and related to the hygroscopic properties of EPS. Some authors, such as Colica et al. (2014), Kidron et al. (1999), Malam Issa et al. (2009) and Xiao et al. (2019), detected a decreased water infiltration and increased run-off due to cyanobacterial EPS. This would be related to the hydrophobic nature of the cyanobacterial compounds, preventing quick wetting of microbial crusts and reducing porosity. Hydrophobic components could also, in our case, explain the slower capillarity. However, others, including Rossi et al. (2012), detected the opposite: an increased water infiltration and hydraulic conductivity as EPS would facilitate water movement by creating micropores and forming new waterways.

The induced changes in water transport and retention might be limited but could impact stone alteration. According to McCabe

et al. (2015), these changes would lead to water accumulation after each wetting event, increasing the depth of the waterfront. This affects deterioration and could trap salts at depth, which might prevent or drive future material loss. Prolonged wetting increases the risk of freeze–thaw weathering (Siegesmund & Snethlage, 2014) and enhances further colonization (Ortega-Morales et al., 2004; Ramírez et al., 2010). Although biofouling might only affect the water redistribution on a microscale, similar to some biological soil crusts (Keck et al., 2016), as water was still absorbed relatively quickly. However, the reduced capillary absorption rate, together with the induced hydrophobicity, suggested that biofilms obstruct absorption. Biofilms might lead to increased run-off that could become important on e.g., an inclined wall or during intense rain showers where water has little time to be absorbed inside the pores. Thus, biofilms could act as natural waterproofing and play a protective role by reducing mineral dissolution, salt weathering and freeze–thaw scattering (Polson et al., 2002). This could be valuable, as the biofilms seemed to have little impact on the water transport properties.

Biofilms can also directly affect building stones. The observation of ESEM of swelling and shrinking, combined with the movement of a potential grain (Figure 5 and online Supplementary Material), suggested that biofilms can potentially mechanically deteriorate natural building stones, just like clays (Fontaine et al., 2015; Wangler & Scherer, 2008). This was already suggested by Dornieden et al. (2000) and Warscheid (1996), but ESEM was able to visualize this process in real time. The video included in the online Supplementary Material showed that smaller RH changes also affect the dimensions of the biofilm. During the day, humidity is constantly changing in relation to varying temperatures (day or night) or sudden rain events (Huby et al., 2020). These changes can be large; for example, micro-climatic monitoring by Huby et al. (2020) on the Saint-Remi Basilica in Reims (France) detected a shift in RH of 77% in RH during one day. Day–night cycles suggest that biofilms will at least perform a once-a-day swell and shrinkage cycle. While the effect of one cycle might be small, numerous cycles could have a relevant impact.

The biofilms might also affect the solubility of salts, as SEM and ESEM showed; along with the cells and the EPS, some granular precipitates, appearing brighter on the BSE images, suggest an inorganic composition. These precipitates (Figures 4A and B) were most likely salts of the growth medium as these were detected inside EPS during the examination of the cultures under optical microscopy. EPS might prevent salt dissolution as the samples were submerged in water to dissolve residual salts before microscopy. Another option could be the precipitation of CaCO_3 linked to photosynthesis (Albertano et al., 2000; Danin & Caneva, 1990; Dittrich & Sibling, 2010; Ortega-Morales et al., 2000).

5 | CONCLUSIONS AND FUTURE RESEARCH

Within this research, the impact of biofilms on water transport and retention in building stones was investigated. The effect was small but mostly in agreement with past work from stones and soils. Biofouling reduced the capillarity and drying rate, but increased the moisture content and water vapour sorption and induced near hydrophobic

conditions. No effect could be measured on the gas permeability and water vapour sorption. These changes will most likely have a small effect but could enhance deterioration, including freeze–thaw weathering and salt damage. Moreover, biofilms can potentially enhance physical weathering and affect the solubility of salts. However, biofilms might obstruct water absorption and induce hydrophobic conditions, which could protect the building stone.

Spectrophotometry allowed us to estimate the amount of biofilm, but due to the variability of the water transport properties, biofouling and detachment of the biofilms, it was not possible to quantify the effect of biofilms. This can be resolved if future research determines the water transport properties on the same stone before and after biofouling, and if the amount of biofilm could be quantified. Future research should also focus on the WCA, as the effect of the biofilms on the wettability was significant. It should measure the WCA of biofouled stones preconditioned at different RH, including both dry and wet biofilms. Future research should study the effect of biofilms *in situ* and combine it with laboratory-based experiments. The effect of environmental biofilms is also understudied: they could increase the water content of a building stone due to sorption or increased water retention or reduce the ingress of water due to induced hydrophobicity. Depending on the dominant effect, biofilms could thus enhance or reduce deterioration. Moreover, environmental biofilms might also be better attached. Experiments should include heterotrophic bacteria, as they can be dominant on building stones (Adamiak et al., 2018; Schröer et al., 2020; Tescari et al., 2018) and colonize the inner pore space as well. Biofilms in the field are often not as dense as those cultured for these experiments. However, due to improved attachment and endolithic colonization, it could be possible that these biofilms have a larger impact on the water–stone relationship compared to laboratory experiments. Moreover, weathered building stones should be included as another behaviour is expected, and studies should be performed to assess the effect of biofilms on weathering. At least, experiments should explore the effect of biofilms on the solubility of salts and determine if biofilms can mechanically alter building stones. These should include not only weathering experiments, but the developed pressure induced by swelling of the biofilm should be measured as well.

ACKNOWLEDGEMENTS

Laurenz Schröer received funding via a PhD fellowship of The Research Foundation - Flanders (Fonds Wetenschappelijk Onderzoek (FWO), Research Grant No. 11D4518N and 11D4520N), which also funded the SEM (Grant No. I013118N), and acknowledges its support in financing this research. We want to thank Dr Annick Wilmotte, Soria Delva, Olga Chepurnova and Tine Verstraete for their advice regarding the cyanobacteria, Dr Yuliia Onyshchenko, Koen De Rycker, Peter Cabus and Daniëlle Schram for their help during the experiments and Carrières Feidt, ROCAMAT and BMB for the building stones. Furthermore, we would also like to thank Professor Dr Stephen Louwye, Professor Dr Stijn Dewaele, Professor Dr Nele De Belie, Professor Dr Heather Viles, Professor Dr Carlos Rodriguez-Navarro and Dr Karel Folens for reading and improving this manuscript.

DATA AVAILABILITY STATEMENT

The data that support the findings of this study are available from the corresponding author.

ORCID

Laurenz Schröer  <https://orcid.org/0000-0003-3635-5180>
 Tim De Kock  <https://orcid.org/0000-0001-5096-1473>
 Sebastiaan Godts  <https://orcid.org/0000-0003-2189-2995>
 Nico Boon  <https://orcid.org/0000-0002-7734-3103>
 Veerle Cnudde  <https://orcid.org/0000-0002-3269-5914>

REFERENCES

- Adamiak, J., Otlewska, A., Tafer, H., Lopandic, K., Gutarowska, B., Sterflinger, K. & Piñar, G. (2018) First evaluation of the microbiome of built cultural heritage by using the Ion Torrent next generation sequencing platform. *International Biodeterioration & Biodegradation*, 131, 11–18. Available from: <https://doi.org/10.1016/j.ibiod.2017.01.040>
- Adessi, A., Cruz de Carvalho, R., De Philippis, R., Branquinho, C. & Marques da Silva, J. (2018) Microbial extracellular polymeric substances improve water retention in dryland biological soil crusts. *Soil Biology and Biochemistry*, 116, 67–69. Available from: <https://doi.org/10.1016/j.soilbio.2017.10.002>
- Albertano, P., Bruno, L., D'Ottavi, D., Moscone, D. & Palleschi, G. (2000) Effect of photosynthesis on pH variation in cyanobacterial biofilms from Roman catacombs. *Journal of Applied Phycology*, 12, 379–384. Available from: <https://doi.org/10.1023/a:1008149529914>
- Anagnostidis, K. & Komárek, J. (1988) Modern approach to the classification system of cyanophytes. 3 - Oscillatoriales. *Algological Studies/Archiv für Hydrobiologie, Supplement Volumes*, 50–53, 327–472.
- Berger-Schunn, A. (1994) *Practical Color Measurement: A Primer for the Beginner, A Reminder for the Expert*. Chichester: Wiley.
- Blows, J.F., Carey, P.J. & Poole, A.B. (2003) Preliminary investigations into Caen Stone in the UK: its use, weathering and comparison with repair stone. *Building and Environment*, 38(9–10), 1143–1149. Available from: [https://doi.org/10.1016/S0360-1323\(03\)00075-1](https://doi.org/10.1016/S0360-1323(03)00075-1)
- Camuffo, D. (1995) Physical weathering of stones. *Science of the Total Environment*, 167(1–3), 1–14. Available from: [https://doi.org/10.1016/0048-9697\(95\)04565-1](https://doi.org/10.1016/0048-9697(95)04565-1)
- Cardell-Fernández, C., Vleugels, G., Torfs, K. & Van Grieken, R. (2002) The processes dominating Ca dissolution of limestone when exposed to ambient atmospheric conditions as determined by comparing dissolution models. *Environmental Geology*, 43(1–2), 160–171. Available from: <https://doi.org/10.1007/s00254-002-0640-x>
- Colica, G., Li, H., Rossi, F., Li, D., Liu, Y. & De Philippis, R. (2014) Microbial secreted exopolysaccharides affect the hydrological behavior of induced biological soil crusts in desert sandy soils. *Soil Biology and Biochemistry*, 68, 62–70. Available from: <https://doi.org/10.1016/j.soilbio.2013.09.017>
- Coombes, M.A. & Naylor, L.A. (2012) Rock warming and drying under simulated intertidal conditions, Part II: Weathering and biological influences on evaporative cooling and near-surface micro-climatic conditions as an example of biogeomorphic ecosystem engineering. *Earth Surface Processes and Landforms*, 37(1), 100–118. Available from: <https://doi.org/10.1002/esp.2232>
- Danin, A. & Caneva, G. (1990) Deterioration of limestone walls in Jerusalem and marble monuments in Rome caused by cyanobacteria and cyanophilous lichens. *International Biodeterioration*, 26(6), 397–417. Available from: [https://doi.org/10.1016/0265-3036\(90\)90004-Q](https://doi.org/10.1016/0265-3036(90)90004-Q)
- De Kock, T., Dewanckele, J., Boone, M., De Schutter, G., Jacobs, P. & Cnudde, V. (2013) Replacement stones for Lede stone in Belgian historical monuments. *Geological Society of London, Special Publications*, 391(1), 31–46. Available from: <https://doi.org/10.1144/SP391.9>
- De Muynck, W., Ramirez, A.M., De Belie, N. & Verstraete, W. (2009) Evaluation of strategies to prevent algal fouling on white architectural and cellular concrete. *International Biodeterioration & Biodegradation*, 63(6), 679–689. Available from: <https://doi.org/10.1016/j.ibiod.2009.04.007>
- Deprez, M., De Kock, T., De Schutter, G. & Cnudde, V. (2020) A review on freeze–thaw action and weathering of rocks. *Earth-Science Reviews*,

- 203, 103143. Available from: <https://doi.org/10.1016/j.earscrev.2020.103143>
- Derluyn, H., Dewanckele, J., Boone, M.N., Cnudde, V., Derome, D. & Carmeliet, J. (2014) Crystallization of hydrated and anhydrous salts in porous limestone resolved by synchrotron X-ray microtomography. *Nuclear Instruments and Methods in Physics Research B*, 324, 102–112. Available from: <https://doi.org/10.1016/j.nimb.2013.08.065>
- Dewanckele, J., De Kock, T., Fronteau, G., Derluyn, H., Vontobel, P., Dierick, M., Van Hoorebeke, L., Jacobs, P. & Cnudde, V. (2014) Neutron radiography and X-ray computed tomography for quantifying weathering and water uptake processes inside porous limestone used as building material. *Materials Characterization*, 88, 86–99. Available from: <https://doi.org/10.1016/j.matchar.2013.12.007>
- Dittrich, M. & Sibling, S. (2010) Calcium carbonate precipitation by cyanobacterial polysaccharides. *Geological Society of London, Special Publications*, 336(1), 51–63. Available from: <https://doi.org/10.1144/SP336.4>
- Dornieden, T., Gorbushina, A. & Krumbein, W. (2000) Patina—physical and chemical interactions of sub-aerial biofilms with objects of art. In: Ciferri, O., Tiano, P. & Mastromei, G. (Eds.) *Of Microbes and Art: The Role of Microbial Communities in the Degradation and Protection of Cultural Heritage*. Dordrecht: Kluwer, pp. 105–119.
- Dreesen, R., Cnudde, V., Dusar, M., de Ceukelaire, M., Bossiroy, D., Groessens, E., Elsen, J., De Kock, T. & Dewanckele, J. (2012) In het voetspoor van Camerman: de opmars van de Franse steen in België. In: van Hees, R.P.J., de Clercq, H. & Quist, W.J. (Eds.) *Stenen van Binnen, Stenen van Buiten – Natuursteen in de Jonge Bouwkunst*. Delft: Delftfdigitalpress, pp. 33–63.
- Dunham, R.J. (1962) Classification of carbonate rocks according to depositional textures. In: Ham, W.E. (Ed.) *Classification of Carbonate Rocks -- A Symposium*. Tulsa, OK: American Association of Petroleum Geologists, pp. 108–121.
- Dusar, M., Dreesen, R. & De Naeyer, A. (2009) *Natuursteen in Vlaanderen -- Versteend Verleden*. Dordrecht: Kluwer.
- Eldridge, D.J. (2001) Biological soil crusts and water relations in Australian deserts. In: Belnap, J. & Lange, O.L. (Eds.) *Biological Soil Crusts: Structure, Function, and Management*. Berlin: Springer, pp. 315–325.
- Elert, K., Ruiz-Agudo, E., Jroundi, F., Gonzalez-Muñoz, M.T., Fash, B.W., Fash, W.L., Valentin, N., de Tagle, A. & Rodriguez-Navarro, C. (2021) Degradation of ancient Maya carved tuff stone at Copan and its bacterial bioconservation. *NPJ Materials Degradation*, 5(1), 44. Available from: <https://doi.org/10.1038/s41529-021-00191-4>
- EN 15802. (2010) Conservation of cultural property - Test methods - Determination of static contact angle.
- EN 16322. (2013) Conservation of cultural heritage - Test methods - Determination of drying properties.
- EN 1925. (1999) Natural stone test methods - Determination of water absorption coefficient by capillarity.
- EN ISO 12571. (2013) Hygrothermal performance of building materials and products - Determination of hygroscopic sorption properties.
- EN ISO 12572. (2016) Hygrothermal performance of building materials and products - Determination of water vapour transmission properties - Cup method.
- Epstein, A.K., Pokroy, B., Seminara, A. & Aizenberg, J. (2011) Bacterial biofilm shows persistent resistance to liquid wetting and gas penetration. *Proceedings of the National Academy of Sciences*, 108(3), 995–1000. Available from: <https://doi.org/10.1073/pnas.1011033108>
- Favero-Longo, S.E. & Viles, H.A. (2020) A review of the nature, role and control of lithobionts on stone cultural heritage: Weighing-up and managing biodeterioration and bioprotection. *World Journal of Microbiology and Biotechnology*, 36(7), 100. Available from: <https://doi.org/10.1007/s11274-020-02878-3>
- Filomena, C.M., Hornung, J. & Stollhofen, H. (2014) Assessing accuracy of gas-driven permeability measurements: A comparative study of diverse Hassler-cell and probe permeameter devices. *Solid Earth*, 5(1), 1–11. Available from: <https://doi.org/10.5194/se-5-1-2014>
- Flemming, H.C., Wingender, J., Szewzyk, U., Steinberg, P., Rice, S.A. & Kjelleberg, S. (2016) Biofilms: An emergent form of bacterial life. *Nature Reviews: Microbiology*, 14(9), 563–575. Available from: <https://doi.org/10.1038/nrmicro.2016.94>
- Folk, R.L. (1962) Spectral subdivision of limestone types. *Bulletin of the American Association of Petroleum Geologists*, 1, 62–84.
- Fontaine, L., Hendrickx, R. & De Clercq, H. (2015) Deterioration mechanisms of the compact clay-bearing limestone of Tournai used in the Romanesque portals of the Tournai Cathedral (Belgium). *Environment and Earth Science*, 74(4), 3207–3221. Available from: <https://doi.org/10.1007/s12665-015-4358-y>
- Fronteau, G. (2000) Comportements telogénétiques des principaux calcaires de Champagne-Ardenne, en relation avec leur facies de dépôt et leur séquençage diagénétique. PhD thesis, Université de Reims Champagne-Ardenne, France.
- Fronteau, G., Schneider-Thomachot, C., Chopin, E., Barbin, V., Mouze, D. & Pascal, A. (2010) Black-crust growth and interaction with underlying limestone microfacies. *Geological Society of London, Special Publications*, 333(1), 25–34. Available from: <https://doi.org/10.1144/SP333.3>
- Gaylarde, C.C., Rodríguez, C.H., Navarro-Noya, Y.E. & Ortega-Morales, B. O. (2012) Microbial biofilms on the sandstone monuments of the Angkor Wat complex, Cambodia. *Current Microbiology*, 64(2), 85–92. Available from: <https://doi.org/10.1007/s00284-011-0034-y>
- Golubić, S., Pietrini, A.M. & Ricci, S. (2015) Euendolithic activity of the cyanobacterium *Chroococcus lithophilus* Erc. In biodeterioration of the Pyramid of Caius Cestius, Rome, Italy. *International Biodeterioration & Biodegradation*, 100, 7–16. Available from: <https://doi.org/10.1016/j.ibiod.2015.01.019>
- Huby, E., Thomachot-Schneider, C., Vázquez, P. & Fronteau, G. (2020) Use of micro-climatic monitoring to assess potential stone weathering on a monument: Example of the Saint-Remi Basilica (Reims, France). *Environmental Monitoring and Assessment*, 192(12), 796. Available from: <https://doi.org/10.1007/s10661-020-08753-w>
- Karimi, M., Mahmoodi, M., Niazi, A., Al-Wahaibi, Y. & Ayatollahi, S. (2012) Investigating wettability alteration during MEOR process, a micro/macro scale analysis. *Colloids and Surfaces B: Biointerfaces*, 95, 129–136. Available from: <https://doi.org/10.1016/j.colsurfb.2012.02.035>
- Keck, H., Felde, V.J.M.N.L., Drahorad, S.L. & Felix-Henningsen, P. (2016) Biological soil crusts cause subcritical water repellency in a sand dune ecosystem located along a rainfall gradient in the NW Negev Desert, Israel. *Journal of Hydrology and Hydromechanics*, 64(2), 133–140. Available from: <https://doi.org/10.1515/johh-2016-0001>
- Kidron, G.J., Yaalon, D.H. & Vonshak, A. (1999) Two causes for runoff initiation on microbiotic crusts: Hydrophobicity and pore clogging. *Soil Science*, 164(1), 18–27. Available from: <https://doi.org/10.1097/00010694-199901000-00004>
- Lebedev, M., Wilson, M.E.J. & Mikhaltsevitch, V. (2014) An experimental study of solid matrix weakening in water-saturated Savonnières limestone. *Geophysical Prospecting*, 62(6), 1253–1265. Available from: <https://doi.org/10.1111/1365-2478.12168>
- Lee, J.B., Radu, A.I., Vontobel, P., Derome, D. & Carmeliet, J. (2016) Absorption of impinging water droplet in porous stones. *Journal of Colloid and Interface Science*, 471, 59–70. Available from: <https://doi.org/10.1016/j.jcis.2016.03.002>
- Lorenz, H. & Lehrberger, G. (2013) Savonnières, Morley & Co.: Oolithische Kalksteine aus Lothringen (Frankreich) als Bau- und Denkmalgesteine in Mitteleuropa. In *19th Engineering Geology Conference*, Munich, 13–16 March; 359–365.
- Macedo, M.F., Miller, A.Z., Dionísio, A. & Saiz-Jimenez, C. (2009) Biodiversity of cyanobacteria and green algae on monuments in the Mediterranean Basin: An overview. *Microbiology*, 155(11), 3476–3490. Available from: <https://doi.org/10.1099/mic.0.032508-0>
- Mager, D.M. & Thomas, A.D. (2011) Extracellular polysaccharides from cyanobacterial soil crusts: A review of their role in dryland soil processes. *Journal of Arid Environments*, 75(2), 91–97. Available from: <https://doi.org/10.1016/j.jaridenv.2010.10.001>

- Malam Issa, O., Défarge, C., Trichet, J., Valentin, C. & Rajot, J.L. (2009) Microbiotic soil crusts in the Sahel of Western Niger and their influence on soil porosity and water dynamics. *Catena*, 77(1), 48–55. Available from: <https://doi.org/10.1016/j.catena.2008.12.013>
- McCabe, S., McAllister, D., Warke, P.A. & Gomez-Heras, M. (2015) Building sandstone surface modification by biofilm and iron precipitation: Emerging block-scale heterogeneity and system response. *Earth Surface Processes and Landforms*, 40(1), 112–122. Available from: <https://doi.org/10.1002/esp.3665>
- Molenaar, N. (1998) Origin of low-permeability calcite-cemented lenses in shallow marine sandstones and CaCO₃ cementation mechanisms: An example from the Lower Jurassic Luxembourg sandstone. In: Morad, S. (Ed.) *Carbonate Cementation in Sandstones: Distribution Patterns and Geochemical Evolution*. Chichester: Wiley, pp. 193–211.
- Ortega-Calvo, J.J., Hernandez-Marine, M. & Saiz-Jimenez, C. (1991) Biodeterioration of building materials by cyanobacteria and algae. *International Biodeterioration*, 28(1–4), 165–185. Available from: [https://doi.org/10.1016/0265-3036\(91\)90041-O](https://doi.org/10.1016/0265-3036(91)90041-O)
- Ortega-Morales, B.O., Narváez-Zapata, J.A., Schmalenberger, A., Sosa-López, A. & Tebbe, C.C. (2004) Biofilms fouling ancient limestone Mayan monuments in Uxmal, Mexico: A cultivation-independent analysis. *Biofilms*, 1(2), 79–90. Available from: <https://doi.org/10.1017/S1479050504001188>
- Ortega-Morales, O., Guezennec, J., Hernández-Duque, G., Gaylarde, C. C. & Gaylarde, P.M. (2000) Phototrophic biofilms on ancient Mayan buildings in Yucatan, Mexico. *Current Microbiology*, 40(2), 81–85. Available from: <https://doi.org/10.1007/s002849910015>
- Polson, E.J., Buckman, J., Bowen, D.G., Todd, A.C., Gow, M.M. & Cuthbert, S.J. (2002) Biofilms on porous building materials: Friend or foe? In *Proceedings of the 9th International Conference on Durability of Building Materials and Components*, Brisbane, 17–20 March; 114/1–114/9.
- Polson, E.J., Buckman, J.O., Bowen, D.G., Todd, A.C., Gow, M.M. & Cuthbert, S.J. (2010) An environmental-scanning-electron-microscope investigation into the effect of biofilm on the wettability of quartz. *SPE Journal*, 15(01), 223–227. Available from: <https://doi.org/10.2118/114421-PA>
- Potts, M. (2001) Desiccation tolerance: A simple process? *Trends in Microbiology*, 9(11), 553–559. Available from: [https://doi.org/10.1016/S0966-842X\(01\)02231-4](https://doi.org/10.1016/S0966-842X(01)02231-4)
- Prieto, B., Silva, B. & Lantes, O. (2004) Biofilm quantification on stone surfaces: Comparison of various methods. *Science of the Total Environment*, 333(1–3), 1–7. Available from: <https://doi.org/10.1016/j.scitotenv.2004.05.003>
- Ramírez, M., Hernández-Mariné, M., Novelo, E. & Roldán, M. (2010) Cyanobacteria-containing biofilms from a Mayan monument in Palenque, Mexico. *Biofouling*, 26(4), 399–409. Available from: <https://doi.org/10.1080/08927011003660404>
- Rindi, F. & Guiry, M.D. (2004) Composition and spatial variability of terrestrial algal assemblages occurring at the bases of urban walls in Europe. *Phycologia*, 43(3), 225–235. Available from: <https://doi.org/10.2216/10031-8884-43-3-225.1>
- Roels, S., Carmeliet, J., Hens, H. & Elsen, J. (2000) Microscopic analysis of imbibition processes in oolitic limestone. *Geophysical Research Letters*, 27(21), 3533–3536. Available from: <https://doi.org/10.1029/1999GL008471>
- Rosenzweig, R., Shavit, U. & Furman, A. (2012) Water retention curves of biofilm-affected soils using Xanthan as an analogue. *Soil Science Society of America Journal*, 76(1), 61–69. Available from: <https://doi.org/10.2136/sssaj2011.0155>
- Rossi, F. & De Philippis, R. (2015) Role of cyanobacterial exopolysaccharides in phototrophic biofilms and in complex microbial mats. *Life*, 5(2), 1218–1238. Available from: <https://doi.org/10.3390/life5021218>
- Rossi, F., Potrafka, R.M., Pichel, F.G. & De Philippis, R. (2012) The role of the exopolysaccharides in enhancing hydraulic conductivity of biological soil crusts. *Soil Biology and Biochemistry*, 46, 33–40. Available from: <https://doi.org/10.1016/j.soilbio.2011.10.016>
- Sawdy, A., Heritage, A. & Pel, L. (2008) A review of salt transport in porous media: Assessment methods and salt reduction treatments. In *Salt Weathering on Buildings and Stone Sculptures*, Copenhagen, 22–24 October; 1–27.
- Schröer, L., Boon, N., De Kock, T. & Cnudde, V. (2021) The capabilities of bacteria and archaea to alter natural building stones – a review. *International Biodeterioration & Biodegradation*, 165, 105329. Available from: <https://doi.org/10.1016/j.ibiod.2021.105329>
- Schröer, L., De Kock, T., Cnudde, V. & Boon, N. (2020) Differential colonization of microbial communities inhabiting Lede stone in the urban and rural environment. *Science of the Total Environment*, 733, 139339. Available from: <https://doi.org/10.1016/j.scitotenv.2020.139339>
- Siegesmund, S. & Snethlage, R. (2014) *Stone in Architecture: Properties, Durability*, 5th edition. Berlin: Springer.
- Smith, B.J., McCabe, S., McAllister, D., Adamson, C., Viles, H.A. & Curran, J.M. (2011) A commentary on climate change, stone decay dynamics and the ‘greening’ of natural stone buildings: New perspectives on ‘deep wetting’. *Environment and Earth Science*, 63(7–8), 1691–1700. Available from: <https://doi.org/10.1007/s12665-010-0766-1>
- Smith, B.J., Warke, P.A. & Curran, J.M. (2004) Implications of climate change and increased “time-of-wetness” for the soiling and decay of sandstone structures in Belfast, Northern Ireland. In: Prikryl, R. (Ed.) *Dimension Stone 2004 – New Perspectives for a Traditional Building Material*. London: Taylor & Francis, pp. 9–14.
- Strunecký, O., Elster, J. & Komárek, J. (2010) Phylogenetic relationships between geographically separate *Phormidium cyanobacteria*: Is there a link between north and south polar regions? *Polar Biology*, 33(10), 1419–1428. Available from: <https://doi.org/10.1007/s00300-010-0834-8>
- Strunecký, O., Komárek, J. & Elster, J. (2012) Biogeography of *Phormidium autumnale* (Oscillatoriales, Cyanobacteria) in western and central Spitsbergen. *Polish Polar Research*, 33(4), 369–382. Available from: <https://doi.org/10.2478/v10183-012-0020-5>
- Tanaka, N., Kogo, T., Hirai, N., Ogawa, A., Kanematsu, H., Takahara, J., Awazu, A., Fujita, N., Haruzono, Y., Ichida, S. & Tanaka, Y. (2019) In-situ detection based on the biofilm hydrophilicity for environmental biofilm formation. *Scientific Reports*, 9(1), 8070. Available from: <https://doi.org/10.1038/s41598-019-44167-6>
- Tescari, M., Frangipani, E., Caneva, G., Casanova Muncicchia, A., Sodo, A. & Visca, P. (2018) *Arthrobacter agilis* and rosy discoloration in “Terme del Foro” (Pompeii, Italy). *International Biodeterioration & Biodegradation*, 130, 48–54. Available from: <https://doi.org/10.1016/j.ibiod.2018.03.015>
- Tomaselli, L., Lamenti, G., Bosco, M. & Tiano, P. (2000) Biodiversity of photosynthetic micro-organisms dwelling on stone monuments. *International Biodeterioration & Biodegradation*, 46(3), 251–258.
- Viles, H.A. & Cutler, N.A. (2012) Global environmental change and the biology of heritage structures. *Global Change Biology*, 18(8), 2406–2418. Available from: <https://doi.org/10.1111/j.1365-2486.2012.02713.x>
- Wangler, T. & Scherer, G.W. (2008) Clay swelling mechanism in clay-bearing sandstones. *Environmental Geology*, 56(3–4), 529–534. Available from: <https://doi.org/10.1007/s00254-008-1380-3>
- Warscheid, T. (1996) Impacts of microbial biofilms in the deterioration of inorganic building materials and their relevance for the conservation practice. *Internationale Zeitschrift für Bauinstandsetzen und Baudenkmalpflege*, 2(6), 493–504. Available from: <https://doi.org/10.1515/rbm-1996-5143>
- Warscheid, T. & Braams, J. (2000) Biodeterioration of stone: A review. *International Biodeterioration & Biodegradation*, 46(4), 343–368. Available from: [https://doi.org/10.1016/S0964-8305\(00\)00109-8](https://doi.org/10.1016/S0964-8305(00)00109-8)
- Warscheid, T., Oelting, M. & Krumbein, W.E. (1991) Physico-chemical aspects of biodeterioration processes on rocks with special regard to organic pollutants. *International Biodeterioration*, 28(1–4), 37–48. Available from: [https://doi.org/10.1016/0265-3036\(91\)90032-M](https://doi.org/10.1016/0265-3036(91)90032-M)
- Xiao, B., Sun, F., Hu, K. & Kidron, G.J. (2019) Biocrusts reduce surface soil infiltrability and impede soil water infiltration under tension and ponding conditions in dryland ecosystem. *Journal of Hydrology*, 568, 792–802. Available from: <https://doi.org/10.1016/j.jhydrol.2018.11.051>

Xiao, B., Zhao, Y.-G. & Shao, M.-A. (2010) Characteristics and numeric simulation of soil evaporation in biological soil crusts. *Journal of Arid Environments*, 74(1), 121–130. Available from: <https://doi.org/10.1016/j.jaridenv.2009.06.013>

SUPPORTING INFORMATION

Additional supporting information may be found in the online version of the article at the publisher's website.

How to cite this article: Schröer, L., De Kock, T., Godts, S., Boon, N. & Cnudde, V. (2022) The effects of cyanobacterial biofilms on water transport and retention of natural building stones. *Earth Surface Processes and Landforms*, 47(8), 1921–1936. Available from: <https://doi.org/10.1002/esp.5355>